NASA TECHNICAL NOTE

NASA TN D-7849

NASA TN D-7849

DECOMPOSITION OF NITRIC OXIDE IN A HOT NITROGEN STREAM TO SYNTHESIZE AIR FOR HYPERSONIC-WIND-TUNNEL COMBUSTION TESTING

John F. Zumdieck and Steven A. Zlatarich

Lewis Research Center

Cleveland, Ohio 44135

NATIONAL AERONAUTICS AND SPACE ADMINISTRATION • WASHINGTON, D. C. • DECEMBER 1974

1. Report No.	2. Government Accession No.	3. Recipient's Catalog No.
NASA TN D-7849		

4. Title and Subtitle	5. Report Date
DECOMPOSITION OF NITRIC OXIDE IN A HOT NITROGEN STREAM TO SYNTHESIZE AIR FOR HYPERSONIC-WIND-TUNNEL COMBUSTION TESTING	December 1974
	6. Performing Organization Code

7. Author(s)	8. Performing Organization Report No.
John F. Zumdieck and Steven A. Zlatarich	E-8031
	10. Work Unit No. 501-24

9. Performing Organization Name and Address	11. Contract or Grant No.
Lewis Research Center National Aeronautics and Space Administration Cleveland, Ohio 44135	
	13. Type of Report and Period Covered
12. Sponsoring Agency Name and Address	Technical Note
National Aeronautics and Space Administration Washington, D.C. 20546	14. Sponsoring Agency Code

15. Supplementary Notes

16. Abstract

A clean source of high-enthalpy air was obtained from the exothermic decomposition of nitric oxide in the presence of strongly heated nitrogen. A nitric oxide jet was introduced into a confined coaxial nitrogen stream. Measurements were made of the extent of mixing and reaction. Experimental results are compared with one- and two-dimensional chemical kinetics computations. Both analyses predict much lower reactivity than was observed experimentally. Inlet nitrogen temperatures above 2400 K were sufficient to produce experimentally a completely reacted gas stream of synthetic air.

17. Key Words (Suggested by Author(s))		18. Distribution Statement
High-enthalpy air	Nitric oxide	Unclassified – unlimited
Synthetic air	decomposition	STAR category 33
Hypersonic wind tunnels	Blowdown facilities	
Supersonic combustion	Pebble-bed heaters	

19. Security Classif. (of this report)	20. Security Classif. (of this page)	21. No. of Pages	22. Price*
Unclassified	Unclassified	28	$3.25

*For sale by the National Technical Information Service, Springfield, Virginia 22151

DECOMPOSITION OF NITRIC OXIDE IN A HOT NITROGEN STREAM TO SYNTHESIZE AIR FOR HYPERSONIC-WIND-TUNNEL COMBUSTION TESTING

by John F. Zumdieck and Steven A. Zlatarich
Lewis Research Center

SUMMARY

Experimental and analytical methods were employed to determine the feasibility of combining nitric oxide with hot nitrogen to cause the high-temperature decomposition of thermodynamically unstable nitric oxide. The desired product of this exothermic reaction was high-enthalpy synthetic air which could be used to simulate Mach 7 to Mach 9 stagnation conditions for supersonic combustion studies. Stagnation temperatures corresponding to these Mach numbers range from 2130 to 3170 K.

A jet of ambient-temperature nitric oxide was injected coaxially into a low-velocity stream of heated nitrogen in a reactor 4.5 centimeters in diameter and 70 centimeters long. Jet velocities were approximately 40 meters per second. The ratio of jet to stream velocity was approximately 6. Gas samples indicating the extent of mixing and reaction were taken near the exit of the duct. Results are compared with one-dimensional chemical kinetics computations.

A chemical kinetics model of the flow which includes the effect of finite mixing rate was developed. Parametric variation of mixing rates produced a variation in the extent of overall reaction. The extent of reaction produced experimentally is also compared with that predicted by the two-dimensional model. Both the one- and the two-dimensional models predict much less reactivity than was observed experimentally. The experiment shows that the overall NO dissociation rate is high enough to achieve conversion to equilibrium in the reactor, provided the inlet nitrogen temperature exceeds 2400 K.

INTRODUCTION

An experiment and an analysis were carried out to determine the feasibility of prc ducing synthetic air by dissociation of nitric oxide in a strongly heated nitrogen strean Success in developing a hypersonic airbreathing engine will depend, to a considerable

extent, upon advances in ground testing techniques. Although high Mach number stagnation conditions can be obtained by vitiation (burning of hydrogen or other fuels in an oxygen-rich airstream), the products will contain excess water vapor or other compounds not present in air. Existing blowdown facilities can produce clean air at stagnation temperatures and pressures high enough to simulate Mach 7 conditions. Above Mach 9, air expanded from stagnation conditions would contain significant quantities of chemically frozen atoms, and thus the composition would be altered and free-flight conditions would no longer be simulated. Ground testing can be utilized in the Mach number range of 7 to 9 only if unusual techniques are devised to generate the extreme stagnation conditions required. These conditions range from 2130 K and 82 atmospheres at Mach 7 to 3170 K and 172 atmospheres at Mach 9.

One such method was proposed jointly by F. E. Belles and R. S. Brokaw of the NASA Lewis Research Center. They suggested the exothermic decomposition of nitric oxide in the presence of strongly heated nitrogen. The 82.0-kilojoule-per-mole heat of reaction will produce a 900 K temperature rise in a completely reacted synthetic air mixture. Preheating of the nitric oxide was also suggested. Through a sequence of intermediate nitric oxide dissociation reactions this scheme could be used to produce synthetic air with nitrogen $\left(N_2\right)$, oxygen $\left(O_2\right)$, and nitric oxide (NO) as the only species appearing in large concentrations during the conversion process.

The decomposition of pure nitric oxide has been the subject of a number of experimental studies. Tests conducted at this Center (ref. 1) and elsewhere (refs. 2 and 3) established a 1300 K temperature limit, beyond which significant dissociation occurs. A feasibility study was prepared (ref. 1) in which chemical-kinetics and heat-transfer calculations were made for a pebble bed sized to heat NO to 1300 K at a flow rate of 8 kilograms per second. This study proposed injection of the heated NO into a nitrogen stream which was to be heated by a separate pebble bed. The total synthetic airflow of 19.6 kilograms per second could supply a Mach 8.5 facility with a 1.2-meter-diameter test section for a 2-minute run. The report concluded with the recommendation that studies of the mixing and reaction of nitric oxide in the presence of heated nitrogen be initiated.

An investigation of dissociation of a nitric oxide jet in a coflowing nitrogen stream was subsequently undertaken. A graphite pebble-bed heater was utilized to heat nitrogen gas. The capacity of the heater was 91 grams of N_2 per second at 2785 K. The hot nitrogen was combined with ambient-temperature nitric oxide in a reactor 4.5 centimeters in diameter and 70 centimeters long. Test pressures ranged from 18 to 26 atmospheres. Jet velocities were of the order of 40 meters per second. The ratio of jet to stream velocity was approximately 6.

Gas samples were drawn and analyzed for NO, N_2, and O_2 content. The inlet flow rates and temperatures and the test section pressure were measured. Flow rates

ranged from 45 to 70 grams per second. Inlet nitrogen temperatures ranged from 2000 to 2400 K.

The extent of reaction measured experimentally was compared with that predicted by an existing one-dimensional computer analysis. A two-dimensional model which includes the effect of finite mixing rate was developed. Predictions from this analysis are also compared with the experimental results.

APPARATUS

The configuration adopted for the test program was one in which high-velocity jet of nitric oxide issued into a circular duct with a coaxial, secondary, low-velocity nitrogen stream. Figure 1 gives a schematic view of the test section. During a test, hot nitrogen gas flowed through a 4.5-centimeter-diameter graphite duct. The NO jet was introduced through a probe with a 5.1-millimeter-diameter opening. At the sampling station, 70 centimeters downstream, gas was drawn off through a sampling probe with a 0.51-millimeter orifice. Downstream of the sampling station the flow expanded to atmospheric pressure through a nozzle with a 6.35-millimeter-diameter throat.

Flow System

The flow system can best be described by considering separately the N_2 and the NO flow branches. A schematic of these flow paths is given in figure 2. Nitrogen gas flowed from a 160-atmosphere supply through the control valves and metering system to the annular space between the heater and the inner pressure vessel wall. The gas then flowed through the pebble bed to the test section and out the nozzle to the exhaust stack.

The graphite pebble bed used to heat the nitrogen gas is shown in a cutaway view in figure 3. The inductively heated susceptor was a graphite cylinder, 25.4 centimeters in diameter and 150 centimeters long, with a 2.54-centimeter-thick wall. (The term susceptor refers to the magnetic coupling characteristic of the heated element, which causes it to behave like a shorted secondary coil of a transformer; resulting eddy currents cause resistive heating.) The susceptor was filled with 0.6-centimeter-diameter graphite balls and wrapped on the outside with a 10-centimeter layer of graphite felt insulation. Outside the insulation was a concentric water-cooled induction heating coil. Power to the coil was supplied from a 3000-cps, 200-kilowatt, motor-generator set. A pressure vessel, designed for 80 atmospheres at 400 K, enclosed the heater. During blowdown an automatic control system regulated the pressurization rate and run pressure.

The nitric oxide supply was contained in 10 standard 23-centimeter-diameter, 142-centimeter-high gas cylinders connected to a common manifold. The 34-atmosphere pressure limit imposed by Federal Transportation Commission regulations on nitric oxide cylinders transported over public highways restricted test pressures to a maximum of 27 atmospheres. The gas cylinder manifold and associated valves and piping were located in a separate building remote from the test cell. The temperature within the building was maintained at 310 K at all times.

As shown in figure 2, a nitrogen purge parallels the nitric oxide system. Either gas could be separately introduced through the injector. At the reactor exit the flow passed through a 6.35-millimeter-diameter supersonic nozzle which exhausted to atmospheric pressure. The flow was vented to the roof of the test facility through a water-cooled exhaust stack 15 centimeters in diameter and 6 meters long.

Gas Sampling and Analysis System

The main features of the gas sampling system are also shown in figure 2. During the nitric oxide injection period, which lasted approximately 30 seconds, two gas samples were drawn. Test gases were chemically frozen by expansion to ambient pressure through a supersonic nozzle in the tip of the sampling probe. Gas flowed continuously through the system during the injection sequence. The pressure in the sampling line downstream of the probe nozzle was maintained at 0.2 atmosphere above ambient by a back-pressure regulator. To obtain the samples, 500-cubic-centimeter evacuated glass bottles, located in the sampling line, were automatically opened and closed in sequence. The first sample was drawn 10 seconds after the beginning of NO injection and the second 10 seconds after the first. The filament of gas constituting the gas sample volume was extracted over the 1-second time interval. This sampling period corresponded to a length interval of 25 test sections at representative reactor gas velocities. At the conclusion of tests, gas sample bottles were removed from the test site to the laboratory for analysis on the following day.

The greatest uncertainty in the results of the gas analysis arose from samples drawn from partially reacted flows. Nitric oxide is a particularly difficult species to measure accurately. Oxygen, formed during high-temperature test runs, reacts with the available nitric oxide to form nitrogen dioxide $\left(NO_2\right)$. This reaction occurs at ambient temperatures in the gas sample bottles and presents an additional problem since it is also difficult to obtain accurate measurements of NO_2. Nitric oxide, N_2, and O_2 concentrations were measured by mass spectrometer; NO_2 concentrations were determined by using ultraviolet absorption techniques.

In addition to the main reactants and products, carbon monoxide, carbon dioxide, and other impurities were present in total amounts of the order of 1 to 2 percent by volume.

Test-Section Details and Instrumentation

The measurements made to supplement the gas sampling results included the nitrogen test-section inlet temperature, the test pressure, the nitrogen flow rate, and the nitric oxide flow rate. Details of the instrumentation are presented in this section.

Special problems in sealing the reactor section were encountered because of the severe thermal expansions and contractions in the heater and test section which arose during heating and blowdown. Figure 4 shows a detailed view of the test section. Close-tolerance slip joints sealed the inlet and outlet ends to prevent cold gas leakage from the annular space between the heater and the pressure vessel. The slip joints permitted the heater and test section to expand axially. (The susceptor lengthened by approximately 3 cm from ambient to run temperature.) Figure 5 shows the thermocouple probe and injector installation. The graphite test section was suspended on the opposing water-cooled stainless-steel probes. Conical graphite surfaces sealed the test section. An alumina sleeve thermally isolated the hot test section from the silicone rubber seal around the probe shank.

A tungsten – tungsten-26-percent-rhenium thermocouple was used to measure the nitrogen gas temperature at the nitric oxide injection station. A tungsten radiation shroud, attached to the end of a water-cooled support jacket, shielded the junction against losses to the surrounding walls. A pressure tap, located in the susceptor dome immediately upstream of the reactor section, facilitated measurement of the test pressure. Venturi meters were used to measure the nitrogen and the nitric oxide flow rates.

A high-pressure, stainless-steel vessel with a 1.33-cubic-meter capacity was charged with water and pressurized with nitrogen gas prior to a run. During tests the tank provided high-pressure water to the cooling passages in the probes, bulkhead, and nozzle.

TEST PROCEDURE

Each experimental run was 5 minutes in length, but 6 to 8 hours were required to prepare for a pair of runs. A chronology of preparatory procedures followed by a description of a typical run might best acquaint the reader with the nature of the tests.

Run Preparation

Unprotected graphite reactor walls were quickly consumed in the oxidizing atmosphere of the reacting flow. To circumvent this problem, removable graphite liners were added (see fig. 6). Liners were segmented as shown to facilitate plasma coating with zirconium oxide refractory. Hot nitrogen, however, reacted with the coating to form zirconium nitride and eventually destroyed the bond between the materials. In spite of this problem, the coating satisfactorily protected the surface from oxidation

throughout the duration of the most severe test runs. The test section could be easily disassembled, and the liners were changed before each set of test runs. Disassembly exposed the heater interior to the atmosphere, so that after reassembly the system was always evacuated to a pressure below 20 newtons per square meter by using a vacuum pump and a liquid-nitrogen cold trap. This procedure sometimes required 2 days, depending on the amount of water vapor the graphite surfaces adsorbed.

Heating times were 4 to 6 hours, depending on the run temperature. Heating rates were minimized to prolong the life of the graphite susceptor. During heating the system was filled with argon gas at a slight positive pressure. Low-pressure water was circulated through cooling passages in the induction coil, nozzle, bulkhead, probes, pressure vessel wall, and exhaust stack during heating. An optical pyrometer, which viewed the susceptor wall through a small hole in the graphite felt insulation, was used to determine the susceptor temperature. When a suitable temperature was reached, the system was placed in a cycling mode pending completion of run preparations.

Run Procedure

To make a test run, power to the heater was removed by shutting down the motor-generator set. The following automatic run sequence was then initiated: The high-pressure water system was pressurized, and flows to the nozzle and probes were established. The cap valve at the exit to the exhaust stack then opened. The main nitrogen flow valve opened, and pressurization of the heater vessel upstream of the nozzle began. The rate of pressurization was controlled by a ramp function generator, and when the run condition was reached, a controller maintained test pressure throughout the blowdown.

During the first 2 to 3 minutes after pressurization the nitrogen gas temperature, measured at the test-section entrance, increased by several hundred degrees because of redistribution of stored energy in the pebble bed. When the nitrogen gas temperature was near a maximum, the nitric oxide injection sequence was initiated.

The injection sequence was divided into three parts; a 1-minute nitrogen lead, a 30-second nitric oxide flow, and finally a 30-second nitrogen purge flow. Adjustments in the nitric oxide flow were made at the beginning of the nitric oxide injection to obtain the proper jet- to main-mass-flow ratios. Two gas samples were taken during the nitric oxide injection period. Completion of the injection sequence coincided with depressurization and run shutdown. When a run was completed, the exhaust stack was closed and resealed, and the heater was again filled with argon gas. Two runs were generally made on a run day, with a 2-hour interval between runs to reheat the pebble bed for the second run.

A 12-hour period was required following the test runs for the apparatus to cool to ambient temperature. Figure 6 also shows the condition of the nozzle, probes, and liners after a typical run day.

ANALYSIS

The analysis of a chemically reacting confined jet is a formidable undertaking. A rigorous approach would involve the simultaneous numerical solution of the complete Navier-Stokes equations, the energy equation, and the individual species equations. Examination of such a difficult general problem from within the framework of our limited objectives was deemed unwarranted. Instead, separate analyses for computations of a nonequilibrium one-dimensional chemical reaction and gas mixing flows were used to study the process. Through appropriate simplifying assumptions these routines were then combined into a single program. The result is a two-dimensional model which gives qualitative insight into the roles of mixing and reaction in the overall process.

One-Dimensional Model

The reaction rate equations describing the dissociation of nitric oxide were introduced into a general chemical-kinetics computer program developed at the Lewis Research Center by Bittker and Scullin (ref. 4). The process was idealized as one-dimensional, constant-area, and adiabatic. The important chemical reactions are given in table I. Reactions VI to VIII are third-body reactions, where M represents the third body. The rate constants and third-body efficiencies used also appear in table I.

The input data to the program include the stream velocity, pressure, and mass fractions of the nitrogen and nitric oxide, which are assumed to be completely mixed, and the mixture temperature. The output of the program is the composition, temperature, and velocity at downstream stations.

Two-Dimensional Model

Although the analogy is incomplete, it is instructive to draw on results from diffusion flame studies in attempting to understand the role of mixing in the overall process being studied. Several investigators have treated the mixing of fuel and oxidant streams by considering diffusion mechanisms only (refs. 5 and 6).

Unfortunately the simple diffusion model cannot be extended directly to the nonisothermal non-constant-velocity case since radial convection terms become significant and must be included in the governing equations. To obtain an accurate description of the flow, a numerical solution to a complete system of equations including the radial momentum equation becomes necessary. To circumvent this difficult problem, a model was devised which includes the principal features of the diffusion model together with

several additional assumptions. The object was to obtain a simple description of mixing upon which chemical reaction could be superimposed. The approach taken was to solve the axial momentum, diffusion, and energy equations with the following assumptions and boundary conditions:

Assumptions:

(1) The radial velocity can be explicitly neglected.

(2) The pressure is constant.

(3) The turbulent eddy diffusivity is constant.

(4) The Prandtl and Schmidt numbers are unity.

(5) The conservation of species equations are strictly satisfied on an integral basis only.

Boundary Conditions:

(1) The jet and main stream velocities are initially equal.

(2) The derivatives with respect to the radial coordinate of all dependent variables are zero on the centerline and at the walls.

The constant-pressure assumption permits the uncoupling of the differential equations. The velocities of the two streams were assumed to be initially equal, and the enhanced mixing due to the presence of a velocity discontinuity in the real flow was accounted for by artificially increasing the value of the turbulent eddy diffusivity.

The equations were solved by using a forward-marching finite-difference technique presented in reference 7. Solving the momentum, energy, and species equations at each axial station while neglecting radial momentum, continuity, and radial convection introduced progressive errors in the species balances. These errors were largest in regions where temperature and species gradients were most severe. A corrective procedure was devised which distributes the species excess or defect in the high-gradient zone according to the relation

$$\left(\dot{m}_{k,j}\right)_{i+1,c} = \left(\dot{m}_{k,j}\right)_{i+1,u} + \frac{r_j\left(\frac{\partial c_k^*}{\partial r}\right)_j}{\sum_j r_j\left(\frac{\partial c_k^*}{\partial r}\right)_j} \Delta\dot{m}_k$$

where $\left(\dot{m}_{k,j}\right)$ and $\left(\frac{\partial c_k^*}{\partial r}\right)_j$ are respectively, the local flux and mass fraction gradient of species k; $\Delta\dot{m}_k$ is the overall mass flux defect of k; and the subscripts u and c refer, respectively, to the uncorrected and corrected local species fluxes at the $i^{th} + 1$ axial station.

Explicitly neglecting the radial velocity v_r guarantees that, at least at the boundaries and centerline, the governing equations are satisfied. This in turn implies that corrections for the absence of radial convection terms need only be introduced in the mixing (or high-gradient) region. The resulting profiles satisfy the integrated conservation of energy, species, and momentum within an acceptable degree of accuracy and exhibit the general features of mixing.

The kinetics program was combined with the mixing scheme, and the two are alternately applied to examine the effect of finite mixing on the overall reactivity of the process. Application of the kinetics program at each radial node for the time period $\Delta z/v_z$ (where Δz is the size of the axial mixing step, and v_z the axial velocity) gives the contributions to the velocity, temperature, and species profiles due to chemical reaction. The turbulent eddy diffusivity was varied over a wide range of values for fixed initial temperature and composition conditions matching those of the experiment.

RESULTS AND DISCUSSION

Experimental Results Compared With One-Dimensional Analysis

Experimental tests were divided into two phases. The first phase included preliminary tests conducted at reduced NO to N_2 flow ratios. The second phase included tests performed with NO to N_2 flow ratios required to produce synthetic air. Figure 7 shows the results of the tests from both phases. (See tables II and III for a complete listing of the experimental data.) The percentage of nitric oxide decomposed

$$\alpha \equiv \frac{\eta_{NO,\,initial} - \eta_{NO,\,sample}}{\eta_{NO,\,initial}} \times 100$$

is plotted in figure 7 as a function of inlet N_2 temperature, where η_{NO} is the NO mole fraction. As the inlet N_2 temperature is increased, α increases until equilibrium composition is attained at the sample station. This behavior is particularly evident in the tests with reduced NO to N_2 flow ratios. Figure 7 also compares experimental results with the one-dimensional analysis. To obtain each computed α value, $\eta_{NO,\,sample}$ in the equation was replaced by $\eta_{NO,\,computed}$ for a reaction time corresponding to the experimental time between injection and sampling. The initial mixture temperatures were varied over a range corresponding to a range of inlet N_2 temperatures. The remaining initial conditions were averages of the experimental values. Scales indicating mixture temperatures for tests from each phase were also presented.

During the first phase NO to N_2 ratios were approximately one-half those required to obtain O_2 to N_2 ratios simulating air. In all the tests significant reaction occurred at nitrogen temperatures well below those which were predicted by the one-dimensional analysis.

Experimental Results Compared With Two-Dimensional Analysis

The assumption of complete mixing in the one-dimensional calculation reduces the mixture temperature below that necessary to sustain significant reaction. To examine the more realistic case of reaction in the mixing zone, the reaction model which includes the effect of finite mixing rate was employed.

Figure 8 shows some typical results obtained from the two-dimensional analysis for three assumed values of eddy diffusivity ϵ. The temperature profiles at axial stations along the duct are for a synthetic air composition with a 2540 K inlet nitrogen temperature and an ambient inlet nitric oxide temperature. The solid lines are profiles obtained by considering the mixing process only. They serve as baselines for the purpose of comparison with results of the mixing-with-reaction program. For the case considered in figure 8(a), the turbulent eddy diffusivity was 9.25×10^{-4} square meter per second. (This value is comparable with values of ϵ found in real jet flows.) Figure 8(a), when compared with figure 8(b) illustrates the effect of doubling ϵ while holding all other initial conditions in the program constant. The amount of nitric oxide dissociated is approximately doubled; this is evident from the increase in area between the solid and the dotted profiles. If ϵ is again increased, this time by 50 percent of the previous value, the amount of reaction is reduced below that experienced in the previous two cases. This can be seen from figure 8(c); the area separating the dashed and the solid lines is smaller.

These results suggest that there exists an optimum reaction-sustaining rate of mixing for the process. Mixing below this rate restricts the reaction and results in mixing-limited reacting flow. Conversely, mixing levels above the optimum tend to quench the stream; a short distance from the inlet plane temperatures throughout the flow field drop to a level such that significant reaction can no longer be supported. The process in this case becomes reaction limited.

The results shown in figure 8 were extended by varying ϵ for a sequence of inlet nitrogen temperatures to obtain a family of curves, each for a constant ϵ. In figure 9 these curves are labeled by the assigned ratio ϵ/ϵ_{opt}, where $\epsilon_{opt} = 1.85 \times 10^{-3}$ square meter per second. The curve labeled ∞ is the one-dimensional kinetics curve for complete initial mixing.

The behavior of these curves further illustrates the interpretation of the mixing- and the reaction-limited regimes. For reaction-limited curves with ϵ/ϵ_{opt} greater than 1 the reaction goes to completion as the N_2 temperatures become sufficiently high. As in the one-dimensional analysis these curves rise steeply with increasing inlet temperature and then abruptly flatten. This behavior contrasts with that shown for curves with values of ϵ/ϵ_{opt} less than 1. These mixing-limited curves rise with increasing slope as the inlet nitrogen temperature is increased until an inflection point

is reached; then for further increases in temperature the slope of the curves decreases. This asymptotic behavior illustrates the effect of a scarcity of reactant in the high-temperature part of the mixing zone.

Although the two-dimensional analysis predicts an optimum mixing rate which shifts the process in the direction of increased reactivity at lower inlet nitrogen temperatures, it too fails to account for the unusually low initiation temperatures observed experimentally.

Experimental and Analytical Mixing Rates

The amount of oxygen present in all forms in the gas sample can be used to determine an equivalent nitric oxide mole fraction. The NO mole fraction that corresponds to complete mixing can be determined accurately from inlet flow measurements. A comparison of these two mole fractions provides a measure of the mixing intensity. The distributions of the difference between these two quantities, for all the gas samples, are shown in figure 10.

Because of the paucity of sampling data it is impossible to draw any firm conclusions regarding mixing rates in the experimental flow. It is likewise impossible to infer an ϵ which would characterize the mixing in the real flow for purposes of comparison with the analysis. However, the mixing data do indicate the order of magnitude of a maximum realistic value for ϵ.

As can be seen from figure 8, turbulent eddy diffusivities greater than ϵ_{opt} are sufficient to eradicate all evidence of the jet over the duct length.

Many of the samples from the experimental flow showed excessively rich or lean nitric oxide concentrations, which suggested that mixing was not so thorough as to destroy all evidence of the jet over the length of the reactor.

The data scatter also suggests that the centerline of the jet might not have been coincident with the duct center during many of the samplings. The possible asymmetry of the jet is further illustrated by the condition of the duct liners depicted in figure 6. A thin carbon layer, deposited during heating and blowdown, was quickly oxidized by the nitric oxide jet. The uneven boundary between light and dark areas on the liners at the injection station delineates the intersection of the jet with the wall.

If the data scatter is evidence of the persistence of an asymmetric jet, ϵ_{opt} represents an upper limit to the turbulent eddy diffusivity of the experimental flow. The valve of ϵ_{opt} employed in the analysis, 1.85×10^{-3} square meter per second, is of the order of magnitude of turbulent eddy diffusivities normally encountered in fully developed turbulent jets.

Discrepancy Between Experiment and Analysis

The one-dimensional analysis predicts N_2 inlet temperatures 300 to 500 K higher than those required experimentally to produce comparable reaction. The two-dimensional model illustrates the effect of finite mixing on overall reactivity but fails to describe the process in the temperature domain of the experimental data. In this section, features of the analysis are examined in greater detail in an attempt to resolve the discrepancy between experiment and analysis. Alternative mechanisms for the increased reactivity are also considered.

One possible source of error in the analysis is the values of the rate constants used in the chemical reaction program. An attempt was made to determine which of reactions in table I had the most significant effect on the overall conversion of NO to N_2 and O_2. The rate constants used throughout this study were preferred values recommended by the authors of references 8 to 10 and are based on a composite of available rate data. The overall conversion rate was most sensitive to the reaction

$$NO + NO \rightarrow N_2O + O \qquad (V)$$

(where N_2O is nitrous oxide) and was sensitive to a lesser extent to the $N_2 + O_2$ and the $NO + O + M$ reactions, IV and VI, respectively.

When the preexponential of reaction V was increased to the forward limit of the error band, the one-dimensional curve for synthetic air was shifted downward in temperature 50 K. However, when an alternative rate expression by Heinrici and Bauer (see ref. 8), based on data from the reverse reaction, was used, a 400 K downward shift was produced. The limiting curve in figure 11 is the result of this adjustment. It suggests that the true set of reaction rates which actually describe the process may give a result which lies anywhere between the preferred curve and this limit curve. It also suggests that it is possible that the finite mixing analysis does describe the flow field in the temperature regime of the experimental data. However, it seems unlikely that uncertainty in the rate constants would be the only cause of such a large discrepancy in the temperature domains.

An alternative explanation for the extensive dissociation at lower temperatures is that it may be caused by fluctuating temperatures within the flow which trigger reaction. The highly nonlinear reactivity-temperature characteristic of the process may produce extensive additional reaction during the positive excursion of a temperature fluctuation.

Another possible mechanism for promoting reaction, not considered previously, is the existence of a recirculation zone downstream of the injector. The probes may serve to stabilize a recirculating flow in a manner analogous to the action of a flameholder.

It is likely that each of the explanations offered accounts in some degree for the unresolved difference between experiment and analysis. However, no quantitative assessment can be made of the magnitude of these effects.

SUMMARY OF RESULTS

The following results were obtained in an experimental and analytical study of the decomposition of nitric oxide in a hot nitrogen stream to synthesize air for hypersonic-wind-tunnel combustion testing:

Ambient-temperature nitric oxide, when mixed with strongly heated nitrogen, rapidly dissociated to form high-enthalpy synthetic air, provided that both the inlet nitrogen temperature and the gas mixing rate were sufficiently high to promote reaction.

A one-dimensional finite-rate chemical kinetics analysis indicated that a 2650 K inlet nitrogen temperature would be required to cause complete dissociation in a reactor of the dimensions used in the experiments. In the test reactor complete dissociation occurred, in some of the test samples, at temperatures of approximately 2200 K.

A reaction model which included the effects of finite mixing rate revealed some interesting qualitative features of the flow but also failed to describe the process in the temperature domain of the experimental data. Three possible explanations were offered for the discrepancy between experiment and analysis. The first involved the uncertainty in the values of the rate constants used in the kinetics analysis. The second suggested the existence of a turbulence-enhanced dissociation mechanism which was not accounted for in the diffusion model. The third postulates a recirculation zone in the flow field.

The experimental data indicated that complete dissociation of a properly mixed flow could realistically be achieved at nitrogen temperatures in excess of 2400 K. Techniques were developed to prevent oxidation of the reactor surfaces while minimizing energy loss through the walls. The practicality of utilizing this concept in future wind-tunnel design, for realizing high Mach number conditions, was demonstrated.

Lewis Research Center,
National Aeronautics and Space Administration,
Cleveland, Ohio, September 9, 1974,
501-24.

REFERENCES

1. Lezberg, Erwin, A.; Zlatarich, Steven A.; and Price, Harold G., Jr.: Feasibility Study of High-Temperature Synthetic-Air Heater for Use With a Mach 8 to 9 Hypersonic Tunnel. NASA TN D-2878, 1965.

2. Yuan, Edward L.; Slaughter, John I.; Koerner, William E.; and Daniels, Farrington: Kinetics of the Decomposition of Nitric Oxide in the Range 700 to 1800°C. J. Phys. Chem., vol. 63, no. 6, June, 1959, pp. 952-956.

3. Kaufman, Frederick; and Kelso, John R.: Thermal Decomposition of Nitric Oxide. J. Chem. Phys., vol. 23, no. 9, Sept., 1955, pp. 1702-1707.

4. Bittker, David A.; and Scullin, Vincent J.: General Chemical Kinetics Computer Program for Static and Flow Reactions With Applications to Combustion and Shock-Tube Kinetics. NASA TN D-6586, 1972.

5. Burke, S. P.; and Schumann, T. E. W.; Diffusion Flames. Industr. Engring. Chem., vol. 20, no. 10, Oct. 1928, pp. 998-1004.

6. Savage, L. D.: The Enclosed Laminar Diffusion Flame. Combustion and Flame, vol. 6, 1962, pp. 77-87.

7. Kurkov, Anatole P.: Mixing of Supersonic Jets Including the Effects of Transverse Pressure Gradient Using Difference Methods. NASA TN D-6592, 1971.

8. Baulch, D. L.; Drysdale, D. D.; Horne, D. G.; and Lloyd, A. C.: Critical Evaluation of Rate Data for Homogeneous, Gas Phase Reactions of Interest in High Temperature Systems. Rept. 4, Dept. Phys. Chem., Leeds University, England, Dec. 1969.

9. Garvin, D.: Chemical Kinetics Data Survey V. Sixty-Six Contributed Rate and Photochemical Data Evaluations on Ninety-Four Reactions. NBSIR-206, National Bureau of Standards, 1973.

10. Garvin, D.: Chemical Kinetics Data Survey IV. Preliminary Tables of Chemical Data for Modeling of the Stratosphere. NBSIR-203, National Bureau of Standards, 1973.

TABLE I.- REACTION RATE CONSTANTS k_j[a]

$$\left[k_j = A_j T^{n_j} \exp\left(-E_j/RT\right)\right]$$

Reaction number, j	Reaction	Preexponential, A_j	Temperature exponent, n_j	Activation energy, E_j J/mole	Reliability of log k_j	Reference
I	$NO + O \rightleftarrows N + O_2$	1.5×10^{9}	1.0	162 192	+0.2	10
II	$O + N_2 \rightleftarrows NO + N$	7.8×10^{13}	0	316 070	±.3	11
III	$O + NO_2 \rightleftarrows NO + O_2$	5.5×10^{12}	0	0	±.06	12
IV	$N_2 + O_2 \rightleftarrows N_2O + O$	6.0×10^{13}	0	434 179	±.4	12
V	$NO + NO \rightleftarrows N_2O + O$	[b]1.3×10^{12}	0	266 997	±.3	11
[c]VI	$NO + O + M \rightleftarrows NO_2 + M$	1.1×10^{15}	0	-7 819	±.08	12
[c]VII	$N + O + M \rightleftarrows NO + M$	6.4×10^{16}	-.5	0	±.2	11
VIII	$M + O_2 \rightleftarrows O + O + M$	2.75×10^{19}	-1.0	496 881	±.3	12

[a]Units of bimolecular and two-body dissociation reaction rate constants are $cm^3/(mole)(sec)$; units of three-body recombination rate constants are $cm^6/(mole^2)(sec)$.

[b]Preexponential value preferred by authors of ref. 8; limiting curve in fig. 11 was obtained by using $A_j = 2.4\times10^{13}$ $cm^3/(mole)(sec)$.

[c]All third-body efficiencies are 1.0 except when M is N_2 in reaction VI and M is N_2O in reaction VII; for these species third-body ratios are 1.40 and 2.25, respectively.

TABLE II.- EXPERIMENTAL DATA FROM REDUCED NITRIC OXIDE TO NITROGEN FLOW RATIO TESTS

Run	Sample	Total mass flux, $\dot{m}_{tot}$, g/sec	Nitrogen mass flux, $\dot{m}_{N_2}$, g/sec	Nitric oxide mass flux, $\dot{m}_{NO}$, g/sec	Inlet nitrogen temperature, T_{in,N_2}, K	Nitrogen velocity, v_{N_2}, cm/sec	Nitric oxide velocity, v_{NO}, cm/sec	Pressures P, atm	Mole fraction difference, $\eta_{NO}-\eta_{NO,mix}$	Nitric oxide decomposed, α, percent
61	1	64.6	50.4	14.2	2322	804	2440	26.6	-3.08×10^{-2}	0.911
61	2	65.9	52.7	13.2	2322	841	2280	26.6	- .13	.892
63	1	65.9	48.6	17.3	2235	750	2990	26.6	2.03	.869
63	2	59.5	44.1	15.4	2235	681	2650	26.6	-3.37	.910
65	1	63.1	44.5	18.6	2037	715	3716	23.3	-10.35	.268
65	2	62.2	44.5	17.7	2029	715	3480	23.3	-6.77	.233
66	1	53.6	36.3	17.3	2156	621	3391	23.3	-7.62	.885
66	2	50.8	34.1	16.8	2148	580	3301	23.3	-8.88	.906
71	1	62.2	47.7	14.5	2100	930	3320	20.0	20.30	.426
71	2	58.2	44.1	14.1	2100	859	3230	↓	15.08	.460
72	1	53.6	37.2	16.3	2140	629	3757	↓	2.20	.920
72	2	51.8	36.3	15.4	2148	619	3548	↓	4.06	.926
73	1	52.3	40.0	12.3	2095	777	2840	↓	-1.30	.628
73	2	53.6	41.3	12.3	2095	807	2840	↓	.05	.705
74	1	59.2	45.5	13.7	2018	846	3140	↓	12.38	.230
74	2	58.2	45.4	12.7	2033	846	2930	↓	12.39	.268
75	1	54.5	40.0	14.5	2193	811	3350	↓	-1.10	.892
75	2	56.8	43.6	13.2	2200	854	3020	↓	1.68	.906
76	2	45.4	30.9	14.5	2139	521	3649	18.3	-.44	.914
77	1	70.8	48.6	22.2	2312	891	3835	26.6	-7.03	.893
77	2	71.7	49.9	21.8	2312	916	3757	26.6	-2.17	.866
83	1	69.6	54.1	15.5	2189	994	3230	22.0	-2.68	.868

TABLE III.- EXPERIMENTAL DATA FROM SYNTHETIC AIR TESTS

Run	Sample	Total mass flux, $\dot{m}_{tot}$, g/sec	Nitrogen mass flux, $\dot{m}_{N_2}$, g/sec	Nitric oxide mass flux, $\dot{m}_{NO}$, g/sec	Inlet nitrogen temperature, T_{in,N_2}, K	Nitrogen velocity, v_{N_2}, cm/sec	Nitric oxide velocity, v_{NO}, cm/sec	Pressures P, atm	Mole fraction difference, $\eta_{NO}-\eta_{NO,mix}$	Nitric oxide decomposed, α, percent
76	1	42.3	26.8	15.5	2140	579	3871	18.3	3.82×10^{-2}	69.0
78	1	62.7	36.8	25.9	2110	612	4693	23.31	1.89	23.4
78	2	61.4	37.7	23.7	2107	628	4633	23.31	-9.28	12.5
79	1	53.2	30.9	22.3	2170	527	4450	23.31	-2.67	92.2
79	2	54.5	32.3	22.2	2170	549	4389	23.31	2.37	90.8
80	1	61.8	32.3	29.5	2240	579	4084	22.97	1.62	86.5
80	2	58.6	35.9	22.7	2250	643	3901	22.97	18.04	77.2
81	1	60.4	37.3	23.1	2348	692	4602	23.31	-6.86	67.5
81	2	58.6	36.4	22.2	2340	673	4359	23.31	10.33	66.3
82	1	61.8	37.7	24.1	2210	661	5181	23.31	39.62	47.4
82	2	58.6	36.8	22.0	2175	634	4359	23.31	14.03	51.9
83	2	63.1	39.5	23.6	2175	731	4876	22.31	-2.64	65.0

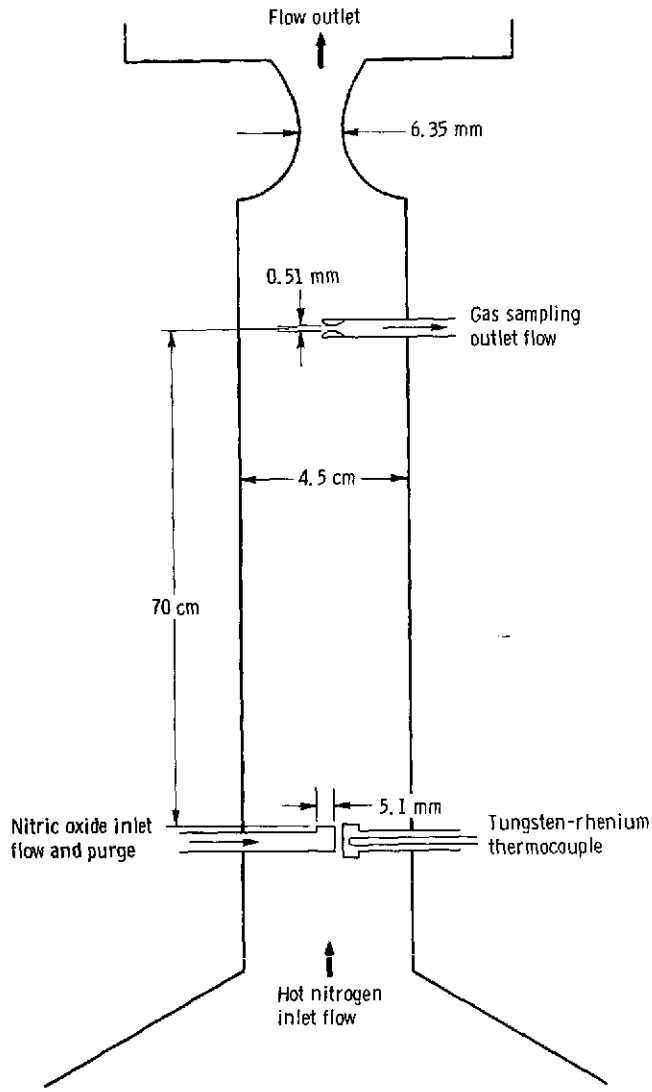

Figure 1. - Experimental configuration.

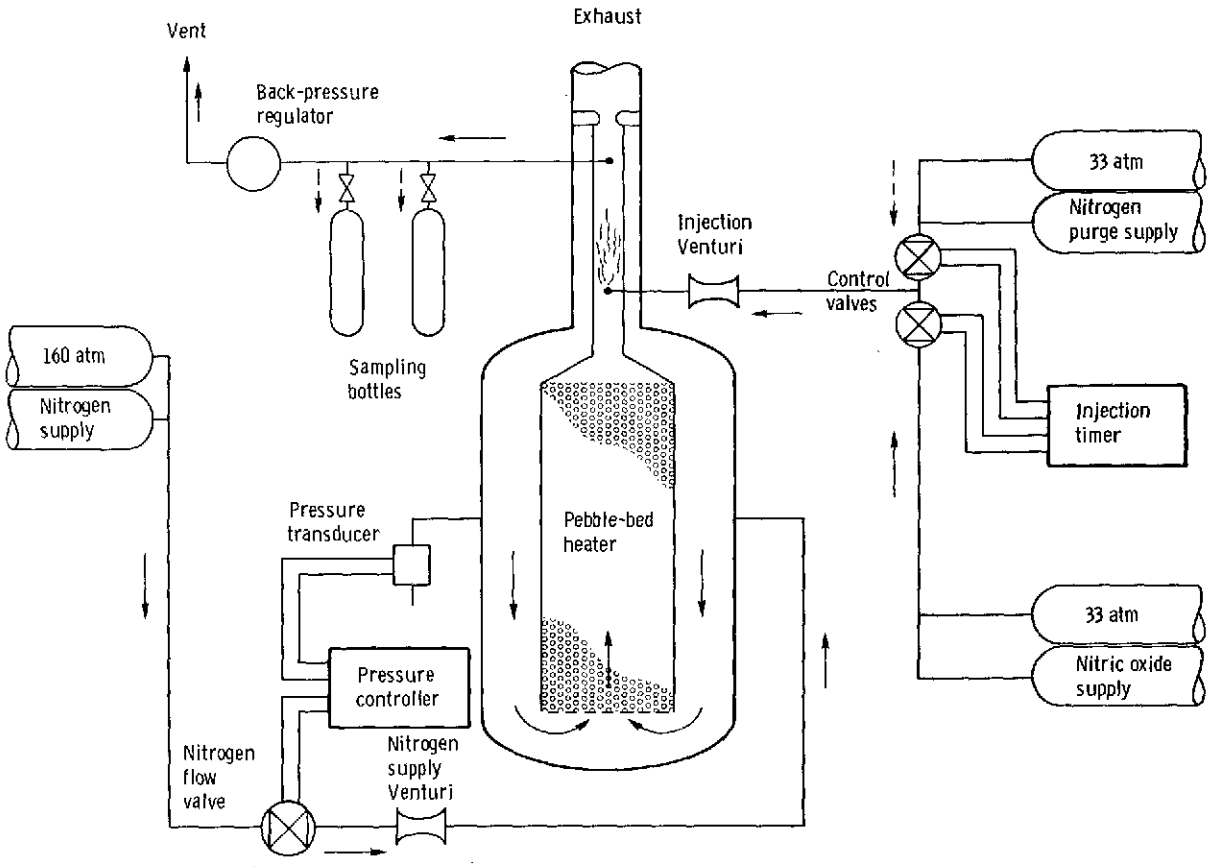

Figure 2. - Gas flow systems.

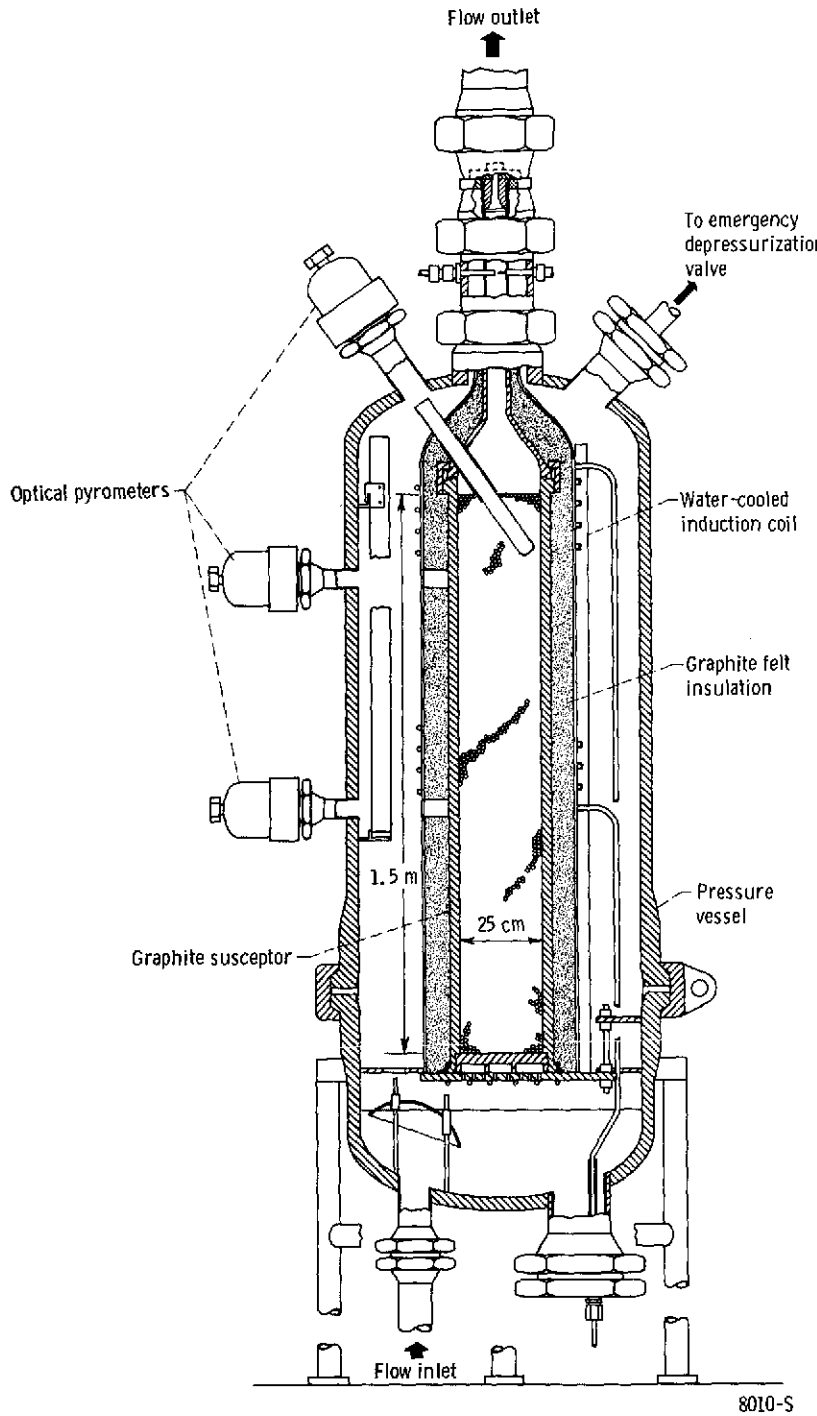

Figure 3. - Cutaway view of graphite pebble bed used to heat nitrogen.

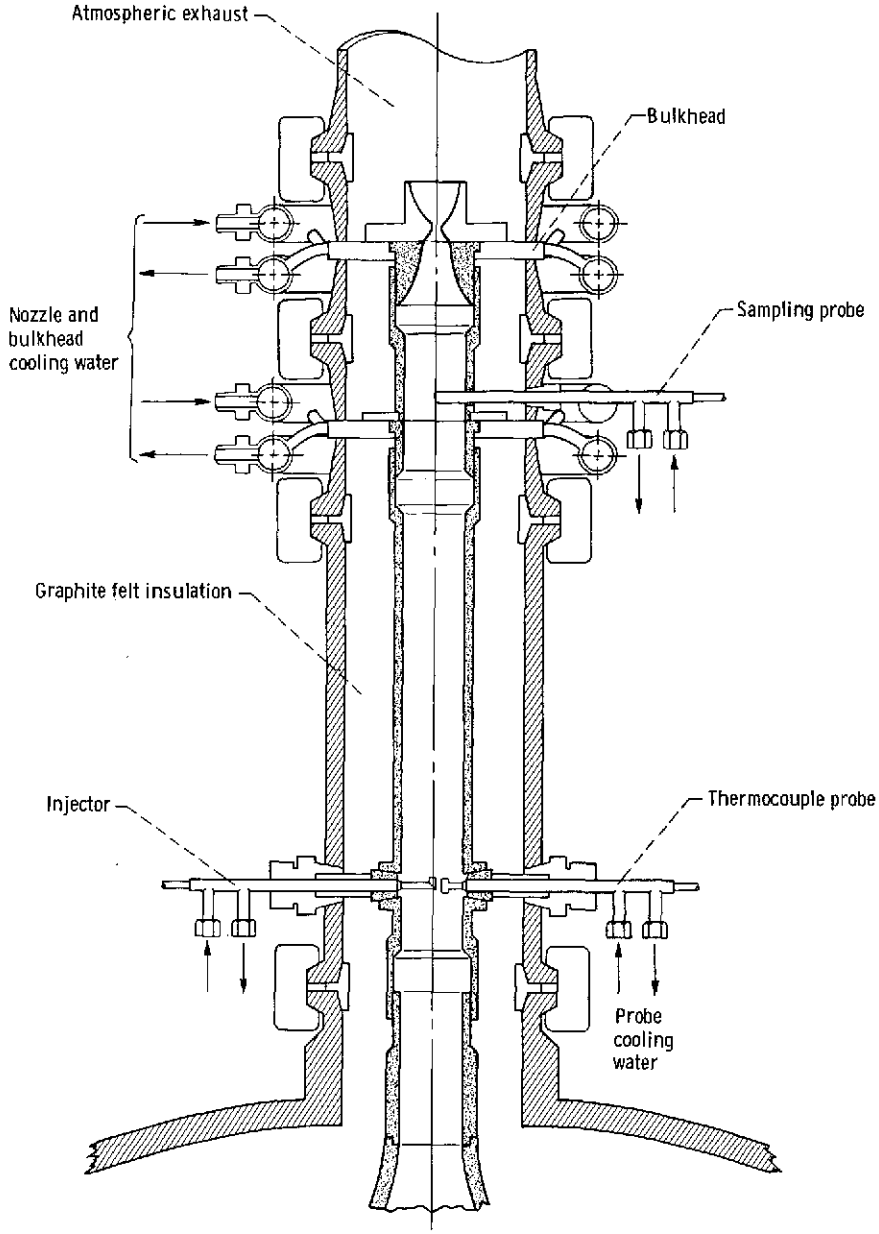

Figure 4. - Test-section detail.

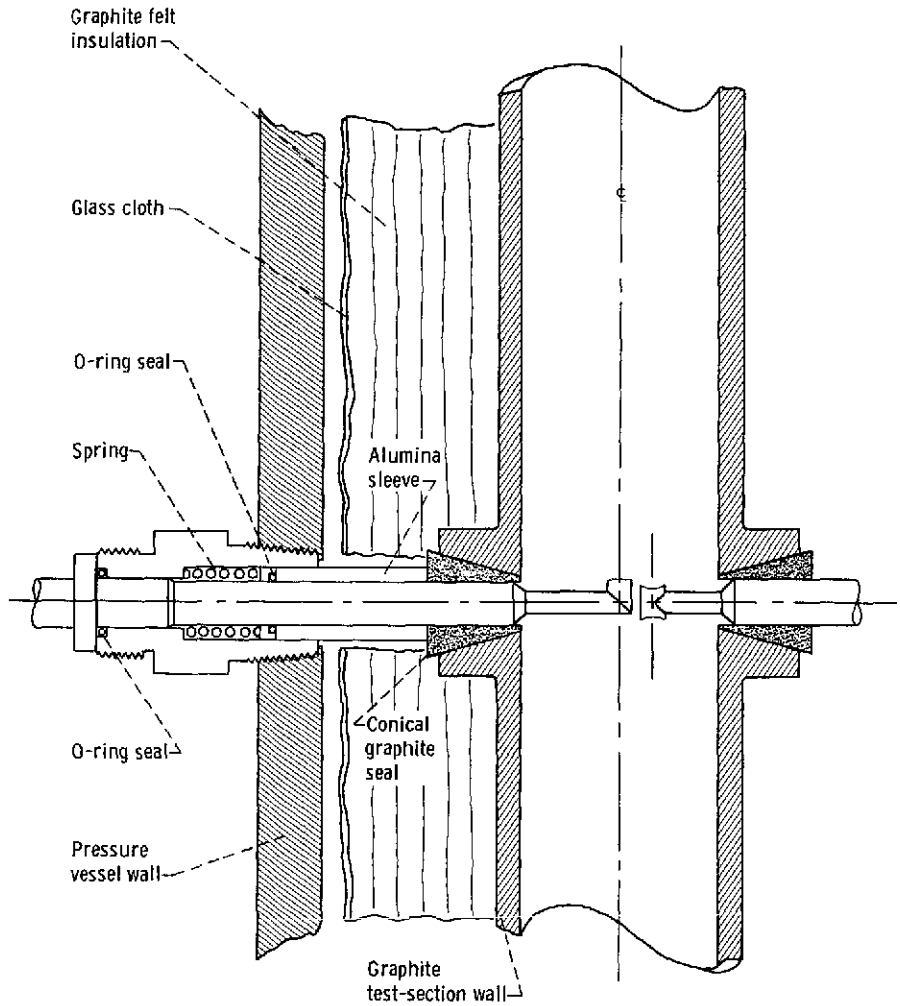

Figure 5. - Probe-assembly detail.

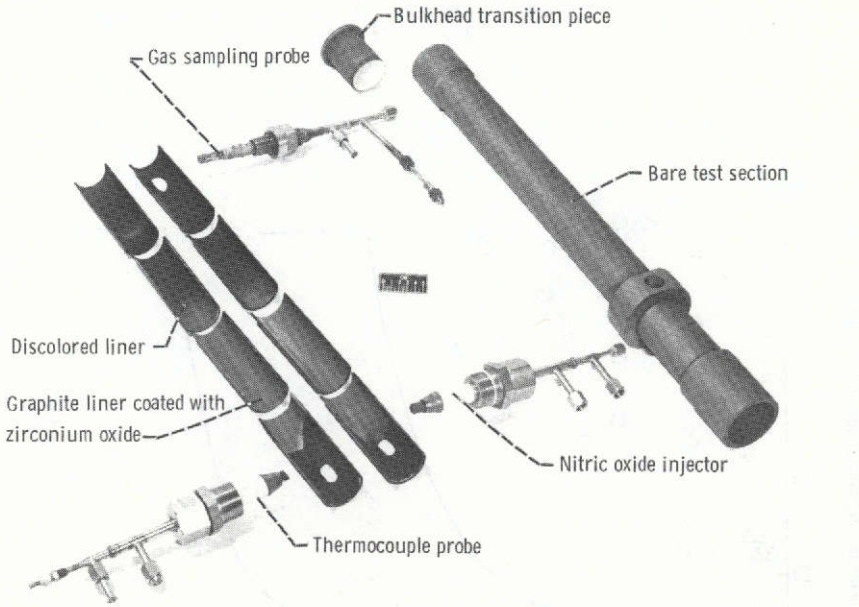

Figure 6. - Probes and liners after typical set of test runs.

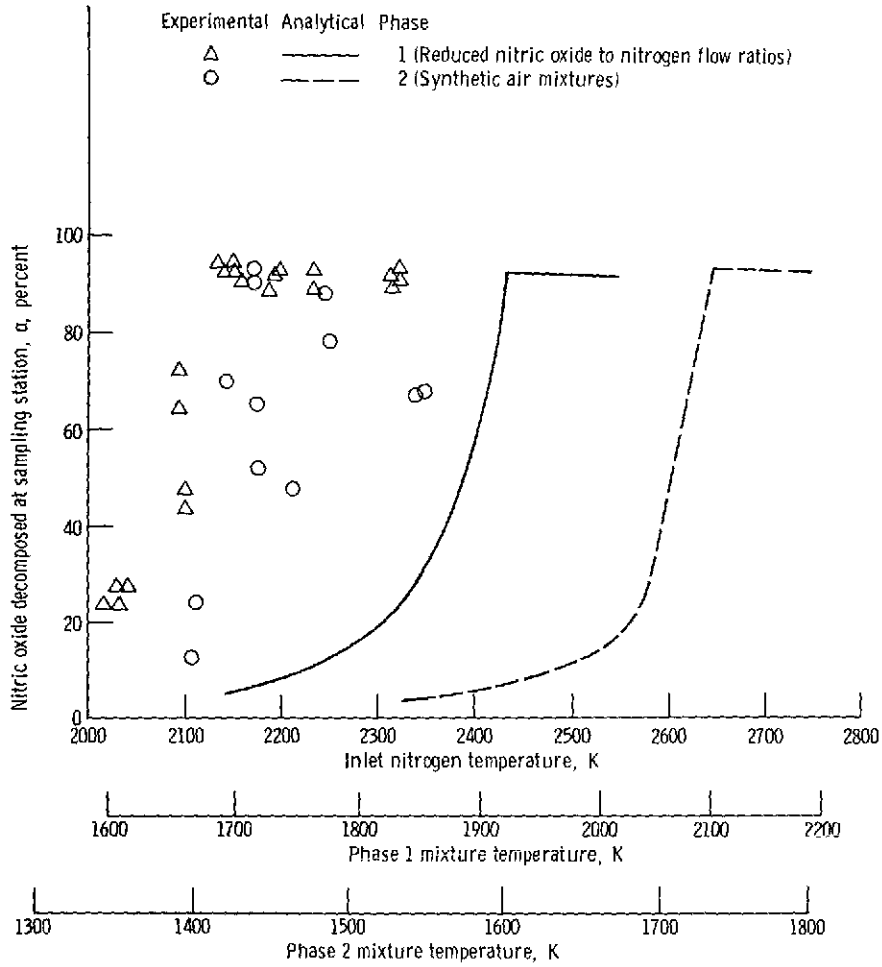

Figure 7. - Experimental results compared with results from one-dimensional finite-rate analysis.

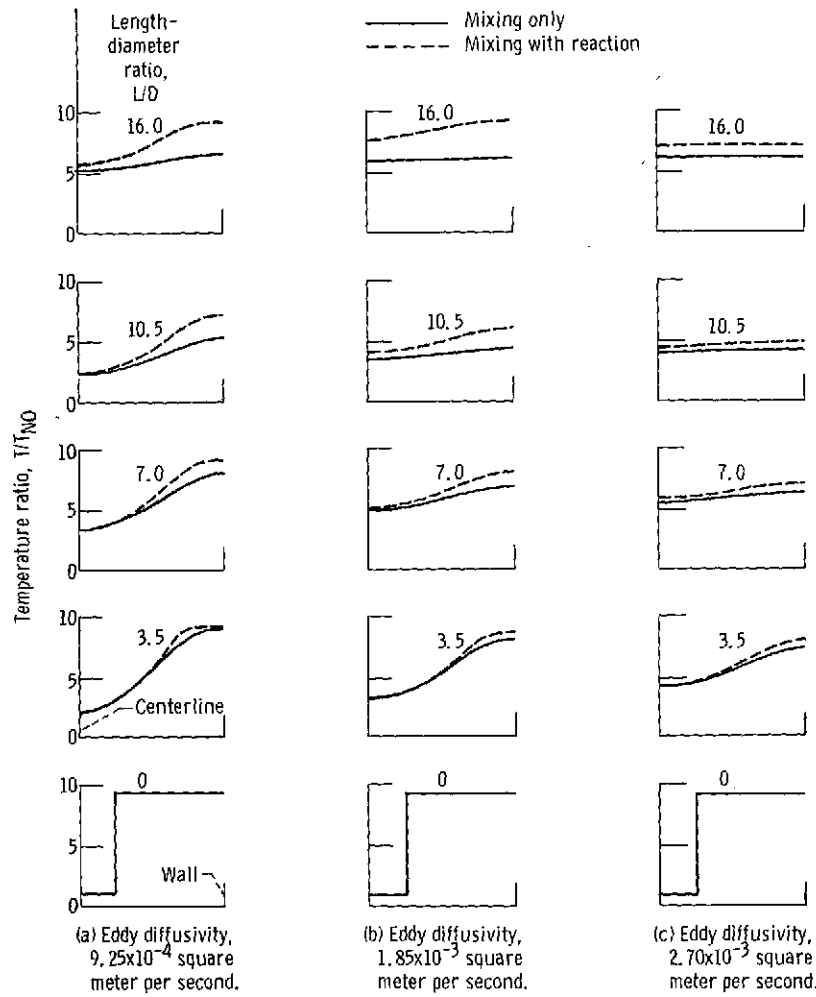

Figure 8. - Temperature profiles for reaction with mixing. Nitric oxide temperature, 273 K; nitrogen temperature, 2540 K; pressure, 23 atmospheres; test-section diameter, 4.5 centimeters.

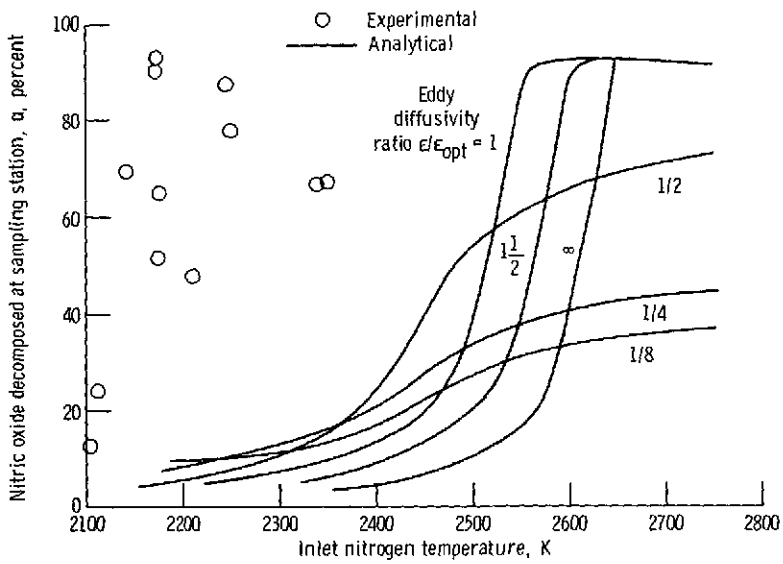

Figure 9. - Experimental results compared with two-dimensional analysis for synthetic air mixtures. Optimum eddy diffusivity, 1.85×10^{-3} square meter per second.

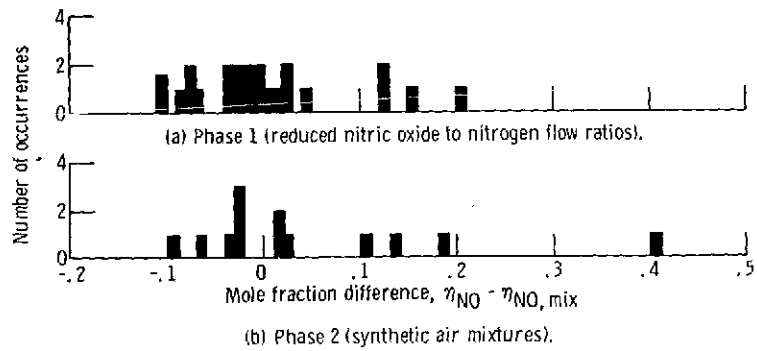

Figure 10. - Mole fraction difference as function of number of occurrences.

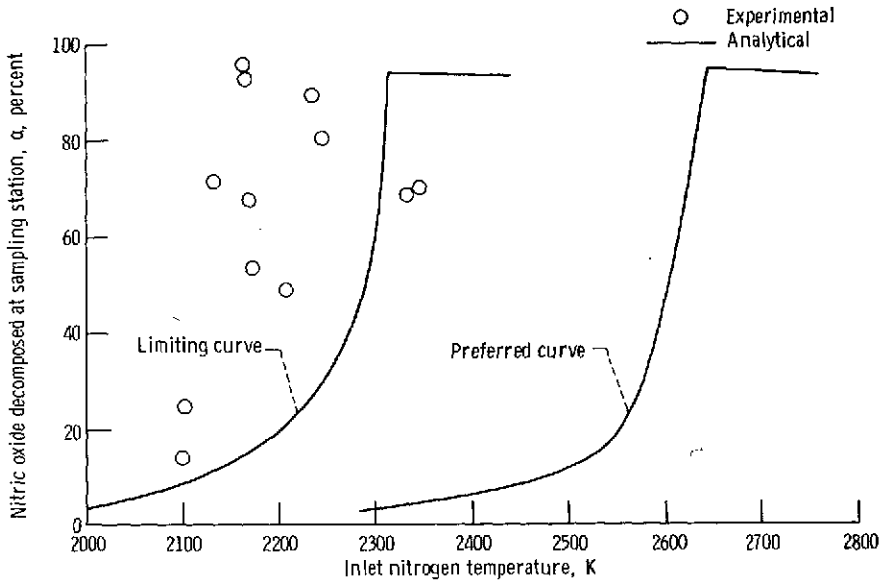

Figure 11. - Preferred and limiting one-dimensional results for synthetic air mixtures.